

# Study of spectral and temporal parameters of superradiance on molecular nitrogen ions in air filament

I.A. Zyatikov, N.G. Ivanov, V.F. Losev, V.E. Prokop'ev

**Abstract.** We report the results of a high temporal resolution study on the formation of superradiance (SR) in plasma on the first negative system of molecular nitrogen ions in plasma of an air filament. The filament is formed by a femtosecond laser pulse with a wavelength of  $\lambda = 950$  nm. For the first time, the actual SR pulse duration at  $\lambda = 428$  nm is measured, which constitutes 1.15 ps (FWHM). According to measurements of a spectral width equal to 0.26 nm, this pulse duration is close to transform-limited (1 ps). It is shown that there is a delay by 6 ps in the SR pulse maximum relative to the pump.

**Keywords:** filament, population inversion, superradiance, femtosecond duration, laser pulse, spectrum, molecule, ions.

## 1. Introduction

Superradiance (SR) in a filament on the first negative system of a molecular nitrogen ion emitting at wavelengths  $\lambda = 391.4$  and 427.8 nm in the forward direction was first obtained in 2011 in pumping by a short and intense IR laser pulse at a wavelength in the mid-IR region ( $\lambda = 1.2\text{--}2.9$   $\mu\text{m}$ ) [1]. For the SR appearance at these wavelengths, additional radiation at the third or fifth harmonic of the pump was used, the wavelength of which coincided with the wavelength of the corresponding transition of the molecular nitrogen ion. Somewhat later, the SR at the specified transitions was observed in pumping by radiation with different wavelengths, namely 800 [2–7], 400 [5], 950 [8, 9] and 1500 nm [10]. In this case, the SR appeared both in the presence of external radiation at the lasing wavelengths [2, 3, 5], and without it [4–6]. In the latter case, it is believed that the radiation of supercontinuum, which occurs in the filament simultaneously with the emission of molecular nitrogen ions, acts as an external triggering pulse. In work [7], the second harmonic radiation with a centre wavelength of 400 nm was used as a triggering signal. It is shown in work [11] that the intensity of SR lines at wavelengths of 391.4 and 427.8 nm depends on the presence of a chirp in the pump pulse. In work [12], it was found that the pump radiation polarisation affects the amplification degree of  $\text{N}_2^+$  radiation in the filament.

I.A. Zyatikov, N.G. Ivanov, V.F. Losev, V.E. Prokop'ev Institute of High Current Electronics, Siberian Branch, Russian Academy of Sciences, Akademicheskii prosp. 2/3, 634055 Tomsk, Russia, e-mail: losev@ogl.hcei.tsc.ru

Received 21 May 2019; revision received 17 July 2019  
Kvantovaya Elektronika 49 (10) 947–950 (2019)  
Translated by M.A. Monastyrskiy

Despite a large number of works dedicated to the study of the properties and conditions of the SR occurrence, the nature of this phenomenon remains unknown. For the present, there are several versions of the appearance of optical amplification in the filament plasma [12–14]. In one of them, it is considered that the excited  $\text{B}^2\Sigma_u^+$  state appears as a result of repeated collisions of electrons with the parent ion [12]. However, it is difficult to explain the presence of a delay in the glow maximum relative to the time moment of exposure. In another version, it is assumed that after multiphoton ionisation, the  $\text{N}_2^+$  ion from the  $\text{X}^2\Sigma_g^+$  ground state transits to the excited  $\text{B}^2\Sigma_u^+$  state due to the absorption of three pump photons [13], but there is no convincing experimental confirmation of this statement. In version [14], it is believed that the population inversion between the  $\text{B}^2\Sigma_u^+$  and  $\text{X}^2\Sigma_g^+$  states arises due to the efficient population of the  $\text{A}^2\Pi_u$  state from the  $\text{X}^2\Sigma_g^+$  state in the interaction of the ion with pump photons. However, radiation on the  $\text{A}^2\Pi_u - \text{X}^2\Sigma_g^+$  transition should appear in this case, which is not observed in practice. There are other versions of the gain implementation on the  $\text{B}^2\Sigma_u^+ - \text{X}^2\Sigma_g^+$  transition, but they are weakly provable.

To understand the nature of SR, it is important to know most fully its characteristics and conditions of its appearance. The most common methods for measuring the SR temporal profile with subpicosecond resolution, such as pump-probe or cross-correlation techniques, do not allow the shape of the amplified radiation pulse to be correctly measured. In the pump-probe method [15], amplified radiation of short duration passes through the filament plasma at various time moments. The total amplification pattern in time reflects the temporal behaviour of only the inverse population at the  $\text{B}^2\Sigma_u^+ - \text{X}^2\Sigma_g^+$  transition. In the cross-correlation method [12, 16], the sum frequency signal is recorded when the pump radiation and SR are added together in a nonlinear crystal. Herewith, as is well known, the process of generating the sum frequency is nonlinear. As a result, the temporal profile of the radiation pulse of sum frequency differs from the SR pulse profile. Note that the characteristic times measured by these methods constitute units and tens of picoseconds, which means that the real time shape of the radiation pulse can only be measured using a streak camera with high temporal resolution. The maximum temporal resolution in recording the glow of nitrogen ions was demonstrated in work [17], where a streak camera with a temporal resolution of 30 ps was used, which is crucially insufficient for the correct measurement of the SR pulse duration.

This paper presents the results of studies of the spectral and temporal parameters of superradiance on the  $\text{N}_2^+$  ions using a subpicosecond-resolution streak camera with no external triggering signal at the corresponding ion transition.

## 2. Equipmental

To form a laser plasma filament, we used radiation generated by the Start-480 solid-state front end being part of the THL-100 multi-terawatt laser system [18]. The front end includes a Ti:sapphire laser (master oscillator) with a continuous-wave pump laser, a grating stretcher, a regenerative and two multi-pass amplifiers, and a grating compressor. Transform-limited radiation pulses with a centre wavelength of 950 nm, a diameter of 1.5 cm at the  $1/e^2$  intensity level, a duration of 60 fs (FWHM), an energy up to 15 mJ, and a Gaussian intensity distribution were formed at the laser system output. The schematic of the experiment is shown in Fig. 1. The filament was formed in the air, with the radiation focused by a lens L1 with a focal length  $F = 165$  mm. The lens was slightly rotated about the beam axis to attach certain astigmatism to its wavefront. In some experiments, the radiation was partially converted in the KDP crystal into the second harmonic (SH). The SH radiation served as a temporal reference point, and was used to determine the instrument function of the streak camera.

The spectral composition of the glow produced by the filament was measured both in the direction of pump radiation propagation (SR) and across it (spontaneous emission – SPE). In measuring the spectrotemporal characteristics, we used a Universal Streak Camera C10910 (Hamamatsu) combined with an Acton SpectraPro SP-2300 spectrometer. The camera had two time sweep regimes: fast (minimum duration, 100 ps) and slow (1 ns). The maximum temporal resolution of the streak camera in the single-pulse regime was 0.644 ps. In the pulse accumulation regime, the temporal resolution for 300 pulses increased to 2 ps due to the presence of the streak camera jitter. To reduce it, the camera was triggered by a signal from a pin diode installed next to the spectrometer.

The spectrometer had three interchangeable diffraction gratings with the number of grating grooves of 50, 300 and 1200 per millimetre at the corresponding resolution of 2.65, 0.62 and 0.23 nm. Our measurements were conducted with a grating having 1200 grooves  $\text{mm}^{-1}$ . To compensate for the

delay time of the streak camera sweep unit, laser radiation was passing a distance of about 14 m and only then focused to form a filament. The time-integrated SR spectra were recorded using an Ocean Optics HR4000 spectrometer (190–1100 nm, 0.7 nm). The SPE spectrum was recorded using a Shamrock SR-500i-D1 spectrometer with a resolution of 0.07 nm, combined with an iStar 334T camera of the Andor™ series, with a resolution of 3 ns. When measuring parameter values close to the device resolution, the real parameter  $A$  (pulse duration or spectral line width) was calculated using the formula  $A = (B^2 - C^2)^{0.5}$ , where  $B$  is the measured parameter and  $C$  is the device resolution.

## 3. Experimental results and discussion

As noted above, certain astigmatism was ascribed to the wavefront. In this case, the glowing plasma length in the focal waist region increased, and the glow intensity decreased. The SR on the molecular nitrogen ions was observed in the direction of pump propagation at a certain tilt of the lens. Figure 2 shows a photograph of the glowing plasma in the waist region in the presence of aberration and in its absence. The longitudinal size of the plasma formation in Fig. 2a is 3 mm, and its diameter is 0.3 mm. The SR presence in aberration conditions only is understandable. Indeed, it was shown in work [19] that in the case of tight focusing, there are no molecular lines in the filament plasma glow, and the lines of atoms and their ions dominate. On the contrary, as the focal length of the lens increases, the atomic lines in the spectrum disappear, and only the lines of the molecular nitrogen and its ion remain. The explanation of this dependence is as follows. At short focusing, the plasma concentration reaches extremely high values ( $\sim 10^{18} \text{ cm}^{-3}$ ). As a result, the rate of quenching the formed molecular nitrogen ions becomes so high that they do not have time to glow up. Introducing astigmatism into a focused beam reduces the concentration of electrons in the plasma and increases the length at which amplification is possible.

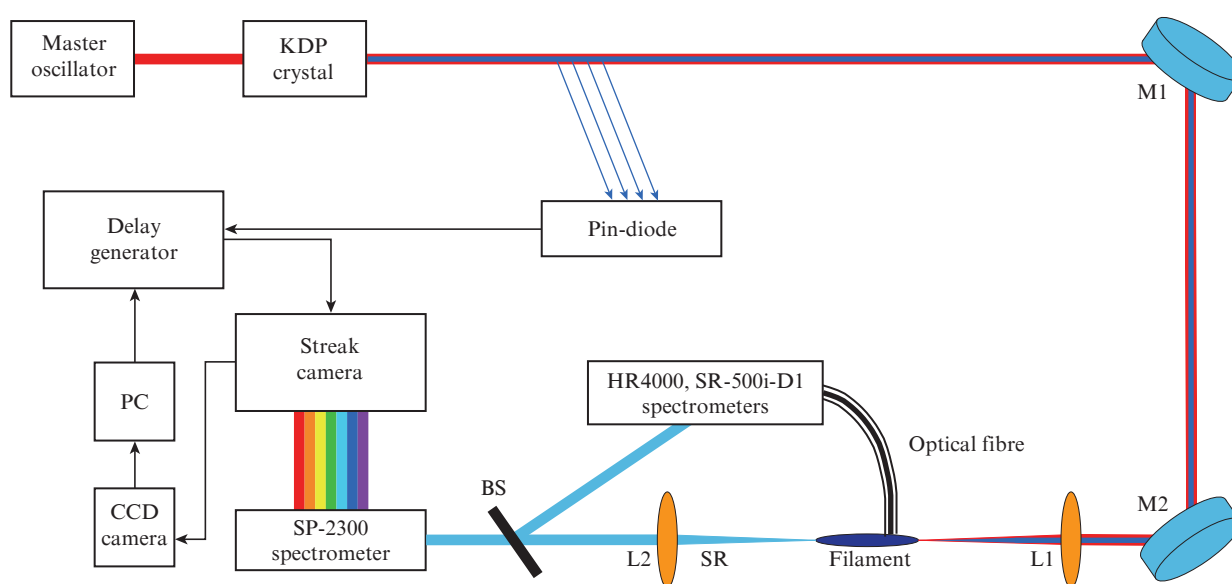


**Figure 1.** Schematic of the experiment: (M1, M2) folding mirrors; (L1, L2) positive lenses with  $F = 16.5$  cm; (BS) beam splitter; (PC) personal computer.

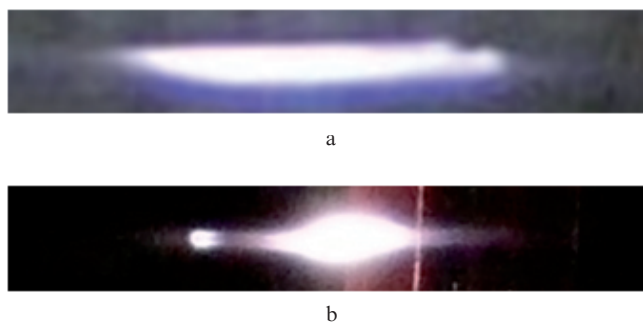


**Figure 2.** Photographs of glowing plasma in (a) the presence and (b) absence of astigmatism in the focused beam. Pump radiation propagates from right to left.

Figure 3a shows the integral SR spectrum taken in the course of pump propagation in the range 370–440 nm. The ratio between the intensities of lines with  $\lambda = 391.4$  and 427.8 nm was regulated by varying the tilt angle of the lens. The line intensity with  $\lambda = 427.8$  nm was maximal when the maximum glow of the filament plasma was located in its anterior. Under certain conditions, other  $B^2\Sigma_u^+ - X^2\Sigma_g^+$  transition lines of the molecular nitrogen ion were also observed: 358.2 (1–0), 388.4 (1–1), and 470.9 (0–2) nm. Note that SR had a significantly greater power and high directivity compared to SPE. Since supercontinuum has always been recorded in the experiment,

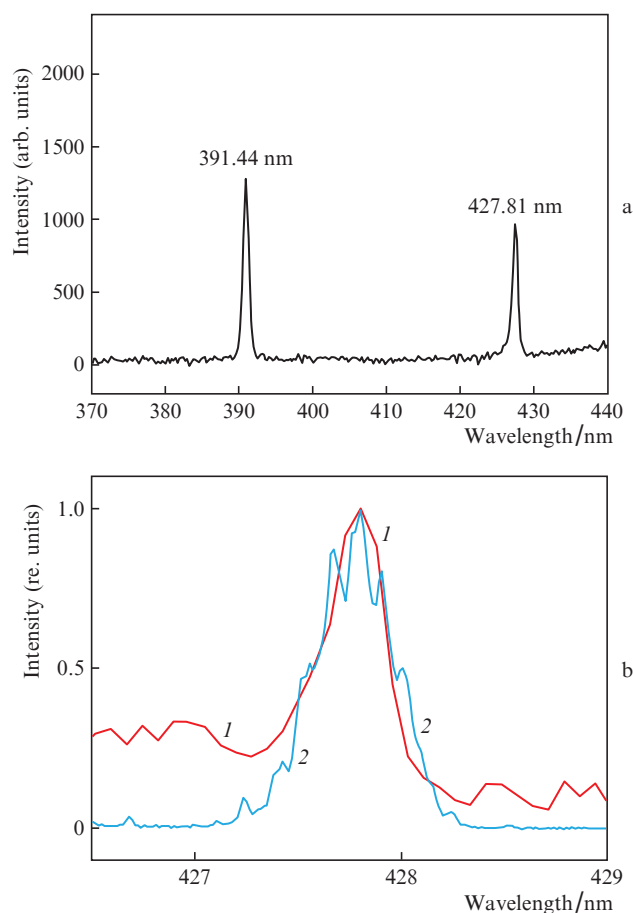


**Figure 3.** Integral spectrum of (a)  $N_2^+$  superradiance lines and (b) (1) SPE and (2) SR spectra at a wavelength of 427.8 nm.

we, like the authors of other works, consider it as a triggering signal for the SR.

Figure 3b displays the SR and SPE spectra at a wavelength of 427.8 nm. It can be seen that the half-widths of the spectra are virtually the same (0.35 nm). However, given the instrument function of the recording device, the half-width of the SR spectrum is 0.26 nm, and that of SPE is 0.34 nm.

The temporal profile of radiation was measured using a Hamamatsu streak camera combined with a spectrometer. In this case, SR was recorded in the single-pulse regime, while SPE was recorded in the accumulation regime in the direction across the filament. In the latter case, pulse sampling regime was used to reduce the temporal spread. Figure 4 demonstrates the time-aligned profiles of the second-harmonic radiation intensity characterising the time moments of exposure, superradiance, and spontaneous emission.

To perform correct measurements, the device was calibrated for recording the second- and third-harmonic radiation, as well as white light [20]. The corrections found in this way were taken into account when constructing the temporal radiation profiles. The SR profile in Fig. 4 reflects the device's instrument function; the start of its intensity growth (zero point) corresponds to the time moment of femtosecond exposure. As can be seen from Fig. 4, the SR intensity maximum lags behind by 6 ps from this time moment. This lasing pulse behaviour can be explained as follows. On the one hand, this is due to the fact that SR corresponds to a narrow-band transition, and, since the pulse duration is inversely proportional to the transition line width, a delay and an increase in the SR pulse duration compared to the pump pulse duration are observed. On the other hand, as is seen from Fig. 4, the maximum intensity of spontaneous emission is delayed by 12 ps relative to the pump pulse, which suggests a slow increase in the population of the upper  $B^2\Sigma_u^+$  state. A sharp drop in the SR intensity after 6 ps can also be caused by the 'removal' of population inversion by the radiation being amplified, while a decrease in the spontaneous emission intensity after 12 ps is caused by quenching of the  $B^2\Sigma_u^+$  level by electrons [3]. The presence of additional maxima in the lasing pulse, which are 4 ps apart, is most likely due to the half-period of rotation of the molecular nitrogen ion, which was also noted in Refs [3, 14, 16].

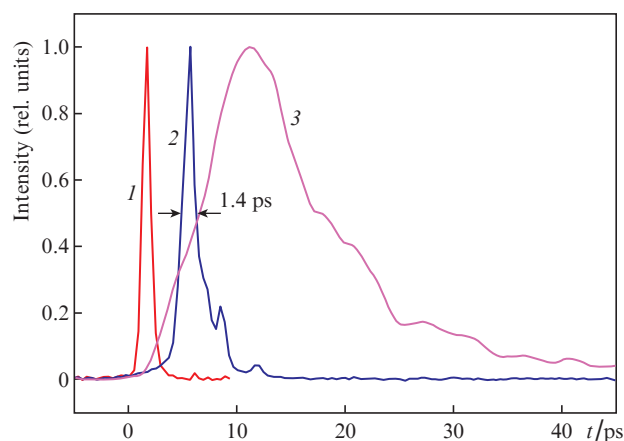


**Figure 4.** Temporal profiles of the pulses of (1) second-harmonic radiation, (2) superradiance, and (3) spontaneous emission at a wavelength of 427.8 nm. Zero time corresponds to the pump pulse arrival.

Given the measured instrument function (0.8 ps), the SR pulse duration is 1.15 ps. Based on the uncertainty relation for the Gaussian pulse shape and the spectrum width of 0.26 nm, we can conclude that the SR duration is close to transform-limited (1 ps).

#### 4. Conclusions

Thus, we have shown that the superradiance pulses on molecular nitrogen ions have a virtually transform-limited duration. This follows from the results of measurements of the pulse duration and its spectral composition. This radiation only occurs under conditions of astigmatism in the pump beam, at which a reduced filament plasma concentration is attained. The delay in the SR intensity maximum at the  $B^2\Sigma_u^+ - X^2\Sigma_g^+$  transition relative to the pump pulse constitutes 6 ps, which is stipulated by the narrow SR line width and slow population growth of the upper  $B^2\Sigma_u^+$  level.

**Acknowledgements.** This work was supported by the Russian Foundation for Basic Research (Scientific Project Nos 19-48-700016 r-sibir' and 18-08-00383 a).

#### References

1. Yao J., Zeng B., Xu H., et al. *Phys. Rev. A*, **84** (5), 051802 (2011).
2. Ni J., Chu W., Jing C., et al. *Opt. Express*, **21** (7), 8746 (2013).
3. Yao J., Li G., Jing C., et al. *New J. Phys.*, **15** (2), 023046 (2013).
4. Liu Yi., Brelet Y., Point G., et al. *Opt. Express*, **21** (19), 22791 (2013).
5. Wang Tie-Jun, Ju Jingjing, Daigle Jean-Francois, et al. *Laser Phys. Lett.*, **10**, 1 (2013).
6. Wang Tie-Jun, Daigle Jean-Francois, Ju Jingjing, Yuan Shuai *Phys. Rev. A*, **88**, 053429 (2013).
7. Helong Li, Hongwei Zang, Yue Su, et al. *J. Opt.*, **19**, 124006 (2017).
8. Prokopiev V.E., Ivanov N.G., Krivonosenko D.A., Losev V.F. *Proc. Conf. 'The Interaction of Highly Concentrated Flows of Energy Materials in Advanced Technology and Medicine'* (Novosibirsk, 2013) p. 6.
9. Prokop'ev V.E., Ivanov N.G., Krivonosenko D.A., Losev V.F. *Izv. Vyssh. Uchebn. Zaved., Ser. Fiz.*, **56** (11), 66 (2013).
10. Azarm A., Corkum P., Polynkin P. *Proc. CLEO: Applications and Technology 2016* (San Jose, CA, US, 2016) paper JTh4B.9.
11. Chenrui Jing, Hongqiang Xie, Guihua Li, et al. *Laser Phys. Lett.*, **12**, 015301 (2015).
12. Yi Liu, Pengji Ding, Guillaume Lambert, et al. *Phys. Rev. Lett.*, **115**, 133203 (2015).
13. Chin S.L., Xu H., Cheng Y., Xu Z. *Chin. Opt. Lett.*, **10**, 013201 (2013).
14. Jinping Yao, Wei Chu, Zhaoxiang Liu, et al. *Appl. Phys. B*, **124**, 73 (2018).
15. Xu H.L., Azarm A., Bernhardt J., Kamali Y., Chin S.L. *Chem. Phys.*, **360**, 171 (2009).
16. Xunqi Zhong, Zhiming Miao, Linlin Zhang, et al. *Phys. Rev. A*, **96**, 043422 (2017).
17. Mingwei Lei, Chengyin Wu, Qingqing Liang. *J. Phys. B: At. Mol. Opt. Phys.*, **50**, 145101 (2017).
18. Alekseev S.V., Aristov A.I., Ivanov N.G., et al. *Laser Part. Beams*, **31** (1), 17 (2013).
19. Ivanov N.G., Losev V.F., Prokop'ev V.E., et al. *Opt. Commun.*, **431**, 120 (2019).
20. Ivanov N.G., Losev V.F., Prokop'ev V.E., Sitnik K.A. *Opt. Commun.*, **387**, 322 (2017).